Bio-Design and Manufacturing (2025) 8:962–975
https://doi.org/10.1631/bdm.2500274

RESEARCH ARTICLE

Pathological quality control chips for tuberculosis

Enru Ye[1] · Jing He[2,3] · Lingna Zhang[1] · Chaofan He[2,3] · Qiuju Zhou[4] · Juan Xu[1] · Meifu Gan[1] · Yong He[2,3]

Received: 26 May 2025 / Accepted: 28 August 2025 / Published online: 25 October 2025

Abstract

Globally, approximately 10 million new tuberculosis (TB) cases are reported annually. Delayed diagnosis due to low detection rates is the primary cause of mortality. Although pathological examination is commonly used for diagnosing TB, 5%–30% of cases remain undiagnosed, emphasizing the urgent need to establish quality control (QC) standards to reduce rates of misdiagnosis and missed diagnoses. To address this, we introduced a novel QC chip for detecting *Mycobacterium tuberculosis* (MTB). A quantitative pathological QC model was constructed by precisely and uniformly integrating MTB and HeLa cells into a photocurable hydrogel. This model was then sliced into uniform sections to create QC chips. It demonstrated that the QC chips exhibited no significant differences in intra-batch or inter-batch variation (coefficient of variation <5%), and remained stable at −80 °C for one year. Furthermore, these chips were found to be 100% effective when tested with 240 clinical samples (200 with special staining and 40 with polymerase chain reaction). In addition to enhancing TB detection rates, this approach offers visualization, quantification, and sustainable production. Overall, this work provides a novel framework for developing QC chips for pathological testing, offering a reliable solution to enhance clinical diagnostic workflows.

Enru Ye, Jing He, and Lingna Zhang have contributed equally to this work.

✉ Juan Xu
xuj4806@enzemed.com

✉ Meifu Gan
ganmf@enzemed.com

[1] Department of Pathology, Taizhou Hospital, Zhejiang University, Linhai 317000, China

[2] State Key Laboratory of Fluid Power and Mechatronic Systems & Liangzhu Laboratory, School of Mechanical Engineering, Zhejiang University, Hangzhou 310027, China

[3] Key Laboratory of 3D Printing Process and Equipment of Zhejiang Province, School of Mechanical Engineering, Zhejiang University, Hangzhou 310027, China

[4] Laboratory Department, Taizhou Hospital, Zhejiang University, Linhai 317000, China

Graphical abstract

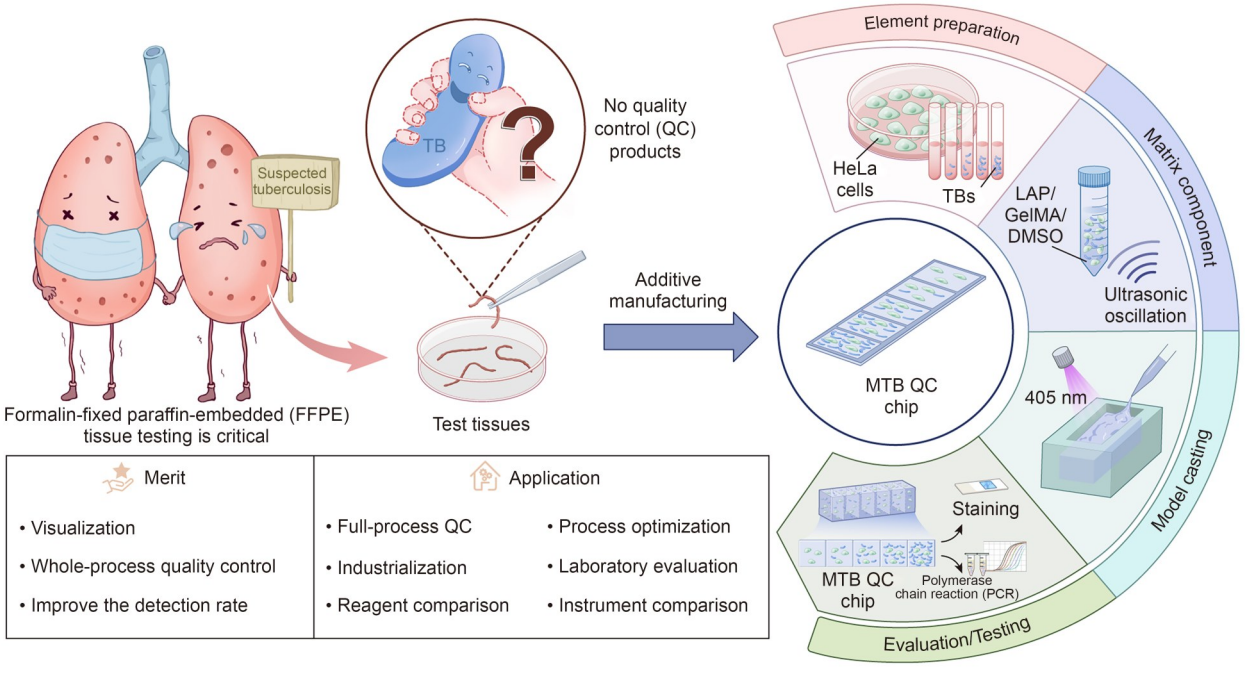

Keywords *Mycobacterium tuberculosis* (MTB) · Pathological model · Quality control (QC) chip

1 Introduction

In 2023, 10.8 million cases of tuberculosis (TB) were reported worldwide, with over 1.2 million deaths annually, as estimated by the World Health Organization (WHO) [1]. In China, approximately 5000 *Mycobacterium tuberculosis* (MTB) pathological tests are conducted per specialized infectious disease hospital annually on average. Pathological tissue sample testing, such as acid-fast bacillus (AFB) staining, is typically used for TB diagnosis, particularly in cases of extrapulmonary TB (accounting for 15%–20%) and pulmonary TB with negative body fluid samples [2, 3]. Despite the efficacy of quantitative polymerase chain reaction (qPCR) tests in detecting MTB, their sensitivity is limited to 50%–84%, which cannot fully meet clinical needs [4, 5]. Clinically, quality control (QC) for MTB pathological testing relies on positive archived formalin-fixed paraffin-embedded (FFPE) tissues. However, the repeatability of FFPE tissues is poor, rendering them suitable only for qualitative validation of special staining of MTB but not for quantitative validation in highly sensitive qPCR testing. This is due to factors such as the uneven distribution of MTB in tissues, low bacterial loads, complexities in tissue processing and preservation, challenges in DNA extraction and purification, and sample contamination that result in approximately 5%–30% of false negatives, false positives, and borderline cases of MTB [6, 7]. Consequently, significant variations exist between laboratories for MTB tests, further impacting clinical decision-making. Moreover, the use of human-derived tissues may raise ethical concerns. Therefore, compared to other clinical samples, MTB pathological tissue testing requires standardized samples for full-process QC to improve detection rates and reduce interlaboratory variability [8].

Previous studies have reported mixing *Escherichia coli* and mouse cells with agar to create simulated FFPE tissues, aiming to evaluate the effects of FFPE processing steps on bacterial DNA detection [8]. However, agar differs significantly from the extracellular matrix (ECM), and its low curing temperature and slow solidification process cause cell and bacterial sedimentation, making it challenging to simulate the precise distribution of small bacterial populations in the ECM. An ideal FFPE-based QC model should feature defined bacterial and host cell loads, clear target values and expected outcomes, a matrix closely resembling the tested tissue, and the ability to participate in the entire experimental workflow.

Recently, organ-on-a-chip technology has emerged as a novel solution for simulating microenvironments, drug testing, and disease modeling [9]. With its highly biomimetic structure and microfluidic advantages, this technology has

significantly boosted precision medicine research. As most host cells die when cocultured with pathogens, pathogen-infected organ models require a highly consistent static structure, which is challenging to construct [10]. Currently, studies on organ-on-a-chip related to MTB infection are lacking. Considering the limitations of existing approaches, we successfully constructed an in vitro QC chip for MTB infection by optimizing materials and processes to create a homogeneous matrix system with rapid shaping, high flowability, and controllable crosslinking. The core challenge lies in accurately loading MTB at different orders of magnitude within a system mimicking the ECM microenvironment, thereby simulating infection samples ranging from borderline to strongly positive. This is essential to ensure the sensitivity and specificity of the reference standard. Additionally, the model must maintain a stable three-dimensional (3D) structure during long-term storage under low temperatures without deformation or denaturation.

In this study, the low-swelling gelatin methacryloyl hydrogel (GelMA, GM-1M) was used as the core skeleton [11], and a whole-genome traceable MTB QC strain served as the quantitative QC product. Dimethyl sulfoxide (DMSO) was used as the low-temperature storage protectant [12], while high-concentration HeLa cells enhanced compatibility with tissue processing procedures. Through ultrasonic mixing and instantaneous crosslinking, an MTB QC model with uniformly dispersed components and long-term storage stability was constructed. Figure 1 shows the fabrication process of the MTB QC chips. Initially, HeLa cells and MTBs were cocultured separately. Subsequently, a defined number of HeLa cells, inactivated MTB, DMSO, and GelMA hydrogel were thoroughly blended and cast into flexible molds to produce the QC models. Following tissue processing and sectioning, QC chips exhibiting negative (TB0), weakly positive to strongly positive responses (TB1–TB4) were obtained. Final histological and molecular biological performance validation demonstrated a structural qualification rate of 90% for the QC models, with robust accuracy and consistency both within and between batches. Moreover, it was stable after one year of storage. The QC chip was effectively implemented in 200 cases of special staining and 40 cases of qPCR detection. The experimental workflow was optimized to ensure precise detection of MTB. In summary, these QC chips provide a standardized framework for MTB detection and can be potentially used to compare the performances of different reagents and detection methods, as well as to reduce interlaboratory variability.

2 Materials and methods

2.1 Cell culture, passaging, and cryopreservation

HeLa cells were kindly provided by Dr. Yong Wang from the College of Life Sciences, Zhejiang University. These cells were cultured in Dulbecco's modified Eagle medium (Gibco, USA) supplemented with 10% (volume fraction) fetal bovine serum, 1% (volume fraction) penicillin, and 1% (volume fraction) streptomycin in a humidified incubator (371, Thermo, USA) at 37 °C with 5% CO_2. Upon reaching ⩾80% confluency, the cells were detached using 0.25% (2.5 g/L)

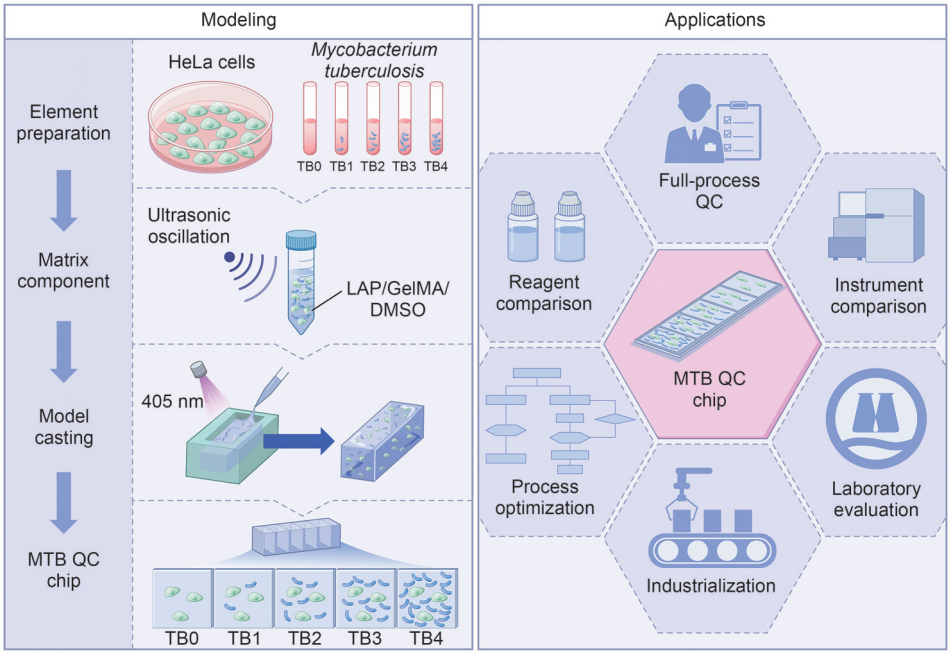

Fig. 1 Development of QC chips for detecting MTB

trypsin and passaged at a 1:3 ratio for expansion. Following trypsinization and centrifugation, the cells were counted using an automated cell counter (IM1200, Countstar, China). Cells were then resuspended in serum-free cell freezing medium and transferred to sterile cryovials for storage at −80 °C.

2.2 *Mycobacterium tuberculosis* culture

The MTB strain (H37Rv) was obtained as a QC strain from the Zhejiang Provincial Center for Disease Control and Prevention. This strain was inoculated onto Lowenstein-Jensen medium using the streak plate method and incubated in a water-jacketed constant temperature incubator (GHP-9270, Shanghai Yiheng Scientific Instrument Co., Ltd., China) for four weeks until colonies appeared. Subsequently, colonies were picked using a cotton swab moistened with 75% (volume fraction) ethanol within a biosafety cabinet (1500TE, HFsafe, China). The colonies were transferred to a centrifuge tube containing 75% (volume fraction) ethanol and inactivated at room temperature for 2 h. Then, the suspension was centrifuged at 10 000 r/min for 5 min, and the pellet was resuspended twice with phosphate-buffered saline (PBS). Subsequently, culture medium was inoculated with an appropriate volume of the inactivated MTB suspension and incubated for two weeks. The absence of colonies indicated successful inactivation. The remaining MTB samples were stored at 4 °C. For flow cytometric analysis, the MTB samples were vortexed and diluted 10-fold. Then, 200 μL of the diluted sample was added to a tube, followed by 2 μL of SYTO9 staining solution, and incubated at 37 °C for 30 min. After analyzing samples using a flow cytometer (Guava EasyCyte, Luminex, USA), the data were analyzed using FlowJo software. The thoroughly mixed MTB suspension was diluted with PBS to four concentrations: 2.784×10^5, 2.784×10^6, 2.784×10^7, and 2.784×10^8 mL^{-1}, and aliquots of 40 μL/tube were prepared and stored at 4 °C for subsequent use.

2.3 Mold fabrication

A resin mold was designed in SolidWorks and fabricated with a projection-based 3D printing (PBP) system (S140, BMF Precision Tech Inc., China). A 10:1 polydimethylsiloxane (PDMS) mixture was injected into the mold and degassed in a vacuum oven to avoid air bubbles. After curing the PDMS at 80 °C for 3 h, it was demolded to yield a PDMS mold with a 2 mm×2 mm×8 mm groove. These molds were sterilized in 75% (volume fraction) alcohol for 1–2 h, followed by three washes with sterile PBS, and then dried.

2.4 Viscosity test

The viscous properties of the 5% (0.05 g/mL) GM-1M and 5% (0.05 g/mL) GM-1M+cells hydrogels were investigated using shear rate sweep measurements (MCR102, Anton Paar, Austria) at a constant shear rate of 10 rad/s and 37 °C. All experiments were repeated at least three times ($n\geqslant3$).

2.5 Tensile test

First, 200 μL of the 5% (0.05 g/mL) GM-1M and 5% (0.05 g/mL) GM-1M+cells hydrogels were both cast into dumbbell-shaped molds (35 mm×2 mm×1 mm). The samples were demolded after curing with 405 nm ultraviolet (UV) light for 60 s. The dumbbell-shaped molds were placed in a universal tensile testing machine (UTM-2203, Shenzhen SUNS Technology Stock Co., Ltd., China) for tensile testing (20 N transducer) at a tensile speed of 2 mm/min. The tensile curves and elongation at break information were obtained. Each group was repeated at least three times ($n\geqslant3$).

2.6 Photorheological tests

Rheological measurements of 5% (0.05 g/mL) GM-1M (EFL-GM-1M, Suzhou Yongqinquan Intelligent Equipment Co., Ltd., China) and 5% (0.05 g/mL) GM-1M+cells hydrogels were performed on a rheometer (MCR302, Anton Paar). Using a 40-mm conical plate (100 μm truncation gap) at 37 °C, 600 μL samples were analyzed at a frequency of 5 rad/s and 1% strain (linear viscoelastic regime) to obtain the storage modulus (G') and loss modulus (G''). Photocrosslinking was initiated using 405 nm UV light, and subsequent rheological changes were monitored in real time.

2.7 Preparation of the matrix system

To prepare a 10% (0.1 g/mL) GM-1M solution, 1 g GelMA was dissolved in 10 mL PBS. Additionally, 0.025 g of lithium phenyl-2, 4, 6-trimethylbenzoylphosphinate (LAP) (Suzhou Yongqinquan Intelligent Equipment Co., Ltd.) was dissolved in GM-1M solution, and the solution was filtered through a 0.22-μm filter for subsequent use. Frozen HeLa cells were thawed at 37 °C and then washed twice with PBS prechilled at 4 °C. After trypan blue staining, the portion of viable cells was counted using a cell counter. Based on the required cell counts of 6.0×10^4 and 6.0×10^6, the appropriate volumes of cell suspension were collected, centrifuged at 800 r/min for 3 min, and washed twice with prechilled PBS under the same centrifugation conditions. After measuring the volume of the cell pellet, 1.2 μL of DMSO, 20 μL of 2.784×10^8 mL^{-1} bacterial suspension, and 60 μL of 10% (0.1 g/mL) GelMA were mixed, and the final volume was adjusted to 120 μL using PBS. The suspension was vortexed for 20 s, ultrasonically mixed for 30 s, and vortexed again for 20 s. The resulting hydrogel matrix systems included a cell-free group and two groups with cell concentrations of approximately 5.0×10^5 and 5.0×10^7 cells/mL, respectively,

which were used to evaluate the effect of cellular content on sectioning quality. After precisely calculating the number of MTB cells required to span C_t values from 26 to 36, we prepared a negative control (TB0) and four positive gradients ranging from weak to strong (TB1–TB4). The final formulation consisted of 10% (0.1 g/mL) DMSO, 5% (0.05 g/mL) GM-1M, and approximately 5×10^7 HeLa cells/mL. The targeted MTB concentrations were 0, 4.63×10^4, 4.63×10^5, 4.63×10^6, and 4.63×10^7 mL^{-1} for TB0−TB4, respectively. After preparation, all matrices were stored at 4 °C until use.

2.8 Casting of matrix

Before the casting process, the matrix system was dissolved in a constant-temperature ultrasonic water bath (SB-300DN, SCIENTZ, China) at 37 °C for 5 min with 3-mm steel balls added to act as resonance sources. The mixture then underwent vortexing for 20 s, sonication for 30 s, and a final vortexing for 20 s to ensure thorough mixing. For each matrix system group, 30 μL aliquots were carefully dispensed into molds, ensuring that no bubbles formed during the process. The constructs were then photopolymerized using a 70-mW light source at a wavelength of 405 nm for 60 s before demolding. The weights of the resulting QC models were recorded. Portions of the TB3 QC models were stored at −20 and −80 °C, separately.

2.9 Tissue processing

The fabricated models were fixed using 4% (0.04 g/mL) paraformaldehyde for 24 h and then weighed. The models were then wrapped in filter paper and processed through a tissue processor (VIP 6AI, Tissue-Tek, Japan) for dehydration, tissue clearing, and paraffin infiltration. The final length of each model was measured using a Vernier caliper. Models with a length of (4.5±0.2) mm and a smooth, crack-free surface were selected for embedding into paraffin blocks using a tissue embedding center (TEC 5, Tissue-Tek).

2.10 Performance verification of QC chips

The reproducibility of the QC chips in histology and molecular biology is crucial for clinical applications. This includes ensuring the consistency of tissue models across various intensity levels within the same batch, within the same positive intensity across different batches, and after storage. To validate intra-batch consistency, three visually qualified models were randomly selected from each of the five groups of tissue models (TB0−TB4). To systematically compare the effects of paraffin embedding versus cryopreservation on the structural integrity and downstream utility of the QC models, aliquots from a single production batch were stored under two conditions: (i) paraffinized and stored at room temperature for 12 months, or (ii) low-temperature conditions (−80 and −20 °C, for 1 month or 12 months, respectively). Each selected model underwent three technical replicates for hematoxylin and eosin (H&E) staining (BaSo, China), AFB staining (BaSo), immunofluorescence (IF) staining (NuoGe, China), DNA extraction (Amoydx, China), and qPCR (Sansure Biotech Inc., China). The TB3 QC chip exhibited a moderate MTB content, faster counting speed compared to TB4, and a smaller counting error than TB1 and TB2. Therefore, this model was used to validate inter-batch consistency, low-temperature storage stability, and stability after paraffin embedding, using the same methods as those for intra-batch consistency assessment.

2.11 Sectioning

The QC models and clinical samples were sectioned into QC chips with uniform thicknesses of 3 and 5 μm using a microtome (RM2235, Leica, Germany). For performance validation, QC-chip sections were obtained at intervals of 50 μm. The 3-μm QC chips were baked in a 70 °C oven for 1 h and then dewaxed in water for histological staining. The 5-μm QC chips were placed in Eppendorf tubes (EPs, eight sections per tube) for qPCR analysis.

2.12 H&E staining

The QC chips were stained with hematoxylin for 8 min, rinsed in water for 5 min, counterstained with eosin for 10 s, dehydrated through a graded ethanol series, cleared in xylene, and mounted with neutral balsam. A pathology slide scanner (SCAN, Pannoramic, Hungary) was used to assess the structural integrity and staining quality of the QC chips, which consisted of cell-free, medium-cell-concentration (approximately 5×10^5 cells/mL), and high-cell-concentration (approximately 5×10^7 cells/mL) matrix systems. This evaluation aimed to determine the appropriate cell concentrations required for constructing TB0–TB4 QC chips.

After H&E staining, scoring was conducted based on four criteria: section flatness, structural integrity, uniform cell distribution, and cavities and cracks, with the score for each individual item being 25 points and a maximum total score of 100 points.

(1) Section flatness: All flat sections were scored 25 points. One point was deducted for each observed uneven section.

(2) Structural integrity: Intact QC-chip structures without significant defects and intact cell structures without fragments were scored 25 points. One point was deducted for each observed fracture or missing structure.

(3) Uniform cell distribution: QC chips with evenly distributed cells without obvious aggregation or sparsity were scored 25 points. One point was deducted for each observed area of nonuniformity.

(4) Cavities and cracks: One point will be deducted for each observed cavity or crack. Absence of cavities and cracks was scored 25 points.

2.13 AFB staining

After applying the anti-acid staining solution, the sections were incubated at room temperature for 15 min and then rinsed with water. Differentiation was performed using acid-alcohol for several seconds, followed by a water rinse. Methylene blue was applied for several seconds to counterstain the background with a light blue color, followed by a water rinse and air-drying. The slides were cleared in xylene and mounted with neutral balsam. The number of MTBs was counted, and images were captured using a microscope (BX43FC, OLYMPUS, Japan).

2.14 Immunofluorescence staining

Reagent A was applied to the QC chips, and the slides were incubated at approximately 25 °C for 15 min, followed by a water rinse. After decolorizing the slides with reagent B for 1 min, the slides were rinsed with distilled water. Then, reagent C was applied for counterstaining for 1 min, followed by rinsing with distilled water. Coverslips were mounted, and the slides were observed under a microscope equipped with a light-emitting diode (LED) filter. MTB appeared as bright orange or yellow-green. The number of MTBs was counted, and images were captured for analysis.

2.15 DNA quality assessment

The tissue chips placed inside centrifuge tubes were dewaxed with xylene and absolute ethanol. Subsequently, 180 μL of buffer DTB and 20 μL of proteinase K solution were added. The tissues were digested at 56 °C for 4 h and then repaired at 90 °C for 2 h. DNA was extracted using a column-based method, and the nucleic acid concentration and OD_{260}/OD_{280} ratio (the ratio of optical density at 260 nm to that at 280 nm) were measured using an ultraviolet–visible (UV–Vis) spectrophotometer (NanoDrop One Microvolume, Thermo Fisher, USA).

2.16 PCR assay

2.16.1 Performance verification with the Sansure Biotech Inc. Kit

The reaction buffer, enzyme mixture, and internal control nucleic acid were thoroughly mixed at appropriate ratios to prepare the PCR master mix. Then, 40 μL of the master mix was dispensed into each well of an eight-well strip. Finally, 5 μL of the extracted DNA sample was added to each well as the PCR template, along with the internal control. The strip was then placed in a real-time PCR instrument (7500, ABI, USA) for amplification and detection using the following cycling conditions: uracil-*N*-glycosylase enzyme reaction at 50 °C for 2 min, Taq enzyme activation at 94 °C for 5 min, followed by 45 cycles of denaturation at 94 °C for 15 s and annealing/extension with fluorescence acquisition at 57 °C for 31 s. The results were subsequently read and analyzed.

2.16.2 Clinical application with the Sinomdgene Technology Inc. Kit

The PCR reaction buffer and primer-probe mixture were thoroughly mixed in the appropriate ratios. Aliquots of 20 μL of the mixture were dispensed into each well of an eight-well strip. Subsequently, 5 μL of the extracted DNA sample was added to each well as the PCR template, along with the internal control. The strip was then placed in a real-time PCR instrument for amplification and detection using the following cycling conditions: uracil-*N*-glycosylase enzyme reaction at 37 °C for 2 min, predenaturation at 95 °C for 3 min, followed by 45 cycles of denaturation at 94 °C for 15 s and annealing/extension with fluorescence acquisition at 60 °C for 35 s. The results were subsequently read and analyzed.

2.17 Statistical analysis

Statistical analysis was performed using SPSS version 25.0. Data in the text are expressed as mean±standard error of the mean. Box and whisker plots show median and interquartile range (minima, 25th percentile, 75th percentile, and maxima). Bar graphs show data as mean±standard deviation. Two-tailed *t*-tests were employed for inter-group comparisons of normally distributed quantitative data and for assessing the storage stability of reference standards. Inter-batch consistency was analyzed using the Wilcoxon test, with a coefficient of variation (CV) <5% indicating low dispersion and no significant difference. Differences were considered statistically significant at p values <0.05 ($^{*}p<0.05$, $^{**}p<0.01$, and $^{***}p<0.001$).

3 Results

3.1 Preparation and characterization of matrix system

Following the WHO guidelines for secondary reference materials, we employed the MTB QC strain (H37Rv) due to its clinical relevance and broad representativeness. This strain was completely inactivated with 75% (volume fraction) ethanol for 2 h (Fig. 2a), as verified by 14-d subculture (no colony-forming unit). The accurate bacterial load was determined by flow cytometry to ensure controlled incorporation into the

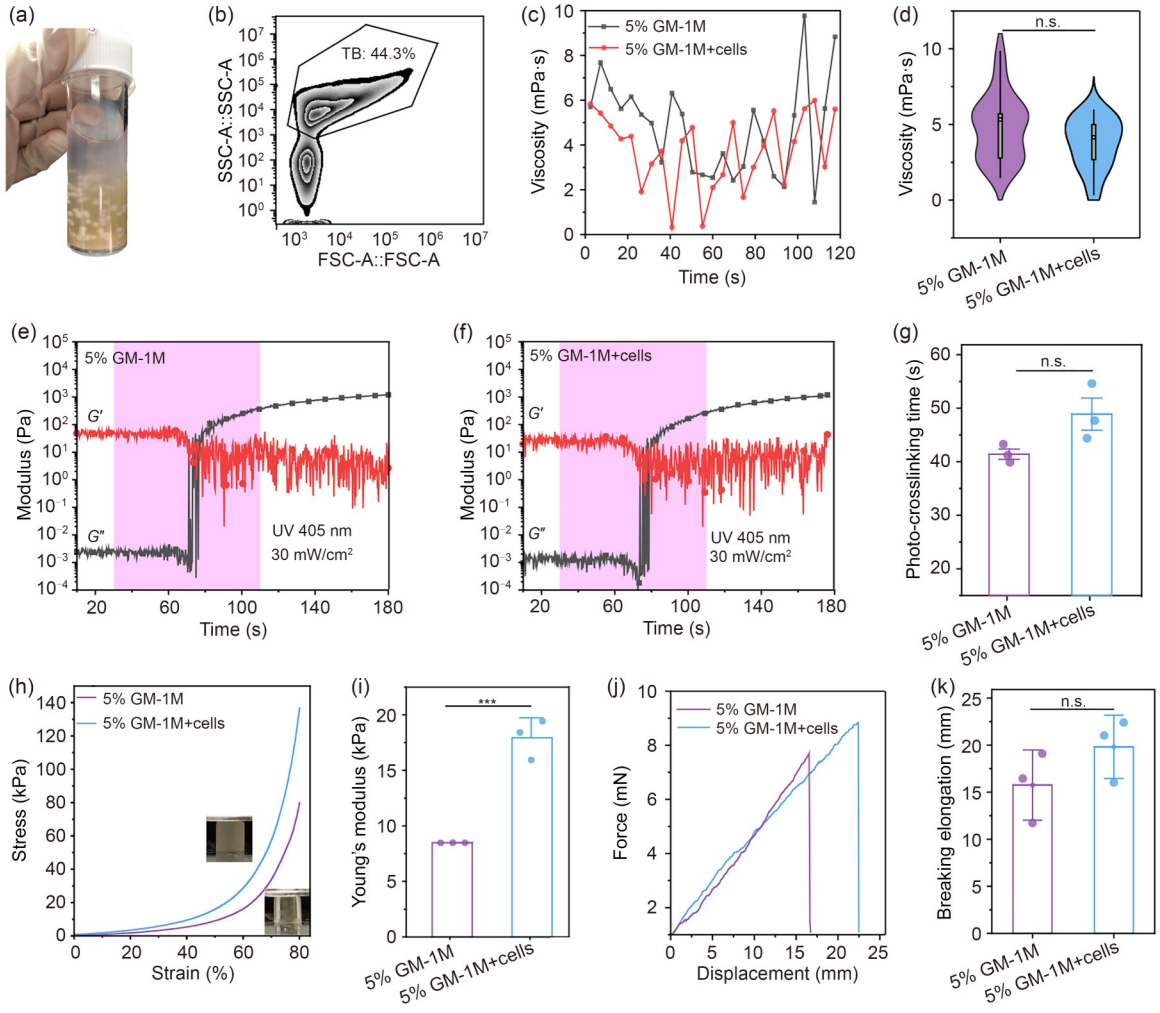

Fig. 2 Properties of the biological matrix. (a) Colony formation after MTB incubation. (b) Counting of MTBs with flow cytometry after inactivation with 75% (volume fraction) ethanol. (c) Viscosity changes. (d) Photo-rheological analysis. 5% GM-1M (e) and 5% GM-1M+cells (f) photo-rheological properties and their curing time changes (g). 5% GM-1M and 5% GM-1M+cells stress – strain curves (h), Young's modulus (i), force–displacement curves (j), and breaking length (k) analysis. Data in (g, i, k) are expressed as mean±standard deviation (n=3). $^{***}p<0.001$; n.s.: not significant

matrix (Fig. 2b). HeLa cells, serving as both an internal PCR control and a cellular mimetic, were coencapsulated along with inactivated MABs in a biocompatible GelMA hydrogel. Previous research had shown that the higher the degree of substitution of GelMA, the denser the molecular network at the same concentration, and the lower the swelling rate. Among these hydrogels, GM-1M, a GelMA variant with 100% amino group substitution, offers advantages such as a low swelling rate and excellent formability. The scanning electron microscopy (SEM) results revealed that the pore area of 5% (0.05 g/mL) GM-1M was at a higher peak (6.9×10^3–7.6×10^3 μm^2) compared to 10% (0.1 g/mL) GM-1M (3.4×10^3–4.1×10^3 μm^2), suggesting a more open porous structure (Figs. S1a and S1b in the supplementary information). However, at high concentrations, GM-1M gels can become overly rigid and prone to fracture after pathological tissue processing. Therefore, to balance formability and brittleness, we selected 5% (0.05 g/mL) GM-1M as the base concentration.

Rheological analysis demonstrated that a high cell density (5×10^7 cells/mL) had a minimal impact on the viscosity of the hydrogel ((4.38±1.76) mPa·s vs. (3.75±1.36) mPa·s, p=0.06; Figs. 2c and 2d). To prevent MTB aggregates, we developed an optimized ultrasonic dispersion protocol at 37 °C (40 kHz with steel-bead resonance) to achieve uniform bacterial distribution while maintaining matrix integrity. Photocuring kinetics studies demonstrated consistent gelation times ((41.40±1.20) s vs. (48.89±3.80) s, p=0.07) with characteristic S-shaped curing profiles (Figs. 2e–2g), confirming that the cellular components had minimal impact on processing. The rapid photocrosslinking capability effectively prevented component sedimentation and ensured homogeneous MTB distribution. The resulting MTB-HeLa-GelMA composite exhibited excellent long-term stability and uniformity,

making it particularly suitable for standardized QC applications in TB diagnostics. Mechanical characterization studies revealed significant material stiffening upon cell incorporation (Young's modulus: (8.47±0.01) kPa vs. (17.93±1.33) kPa, p=0.0008), achieving stiffness comparable to human liver parenchyma (15–20 kPa) (Figs. 2h and 2i). While elongation at break showed no statistically significant difference between groups ((16.07±2.60) mm vs. (20.00±2.44) mm, p=0.64; Figs. 2j and 2k), the cell-incorporated matrix exhibited enhanced resilience, a critical property for QC-chip fabrication that ensures structural integrity during handling and processing.

This optimized system successfully addresses key challenges in reference material development, combining biological relevance with robust physical properties for reliable diagnostic applications. Incorporation of cells enhanced the mechanical properties while maintaining the processing characteristics, representing significant advantages for practical implementation in clinical QC systems.

3.2 Fabrication of the model and QC chips

Inert and nontoxic PDMS flexible molds with internal dimensions of 2 mm×2 mm×8 mm were fabricated using dual molding based on PBP technology. The base system was cast into a model with uniform dimensions, fully cured at 60 s under 405 nm light, and demolded to give a QC model with consistent edge rules and quality ((36.87±0.03) mg), which met the design specifications (Figs. 3a and 3d). The appearance and weight of the QC model ((37.73±0.03) mg) did not change significantly after 24 h of fixation (Figs. 3b and 3d). After dehydration, the long axis and the short axis both contracted by about 50%, and no apparent dissolution, cracking, or structural damage was observed. Based on this, the model was deemed suitable for paraffinization. The appearance pass rate of the QC model after treatment was 90.24% (Figs. 3c and 3e). Structurally intact QC chips with uniform thicknesses of 3 and 5 μm could be obtained continuously at the slicing stage, facilitating high-quality histological analysis for quantitative QC.

3.3 Morphological performance verification of the QC chip

3.3.1 H&E staining visualization analysis

We compared the quality of the sections using the following three matrix systems: the cell-free, medium-concentration (5×10^5 cells/mL), and high-concentration (5×10^7 cells/mL) groups. The results showed that the section flatness of the high-concentration group was the best, and the wrinkle rate and crack density were significantly lower than those of the other two groups (Figs. 4a–4c). Therefore, all subsequent TB0–TB4 gradient QC chips were prepared using the 5×10^7 cells/mL matrix system. The five groups of QC chips, which were prepared and stained with H&E, had smooth surfaces, complete structures, uniform cell distribution, and no voids or cracks. The average scores were all greater than 95 points, meeting the high-quality standards for microarray analysis (Fig. S2 in the supplementary information). The wax block section scores remained unchanged after being stored at room temperature for 12 months (Fig. S3a in the supplementary information). Further investigation of cryopreservation conditions can be made. The −80 °C group was only occasionally

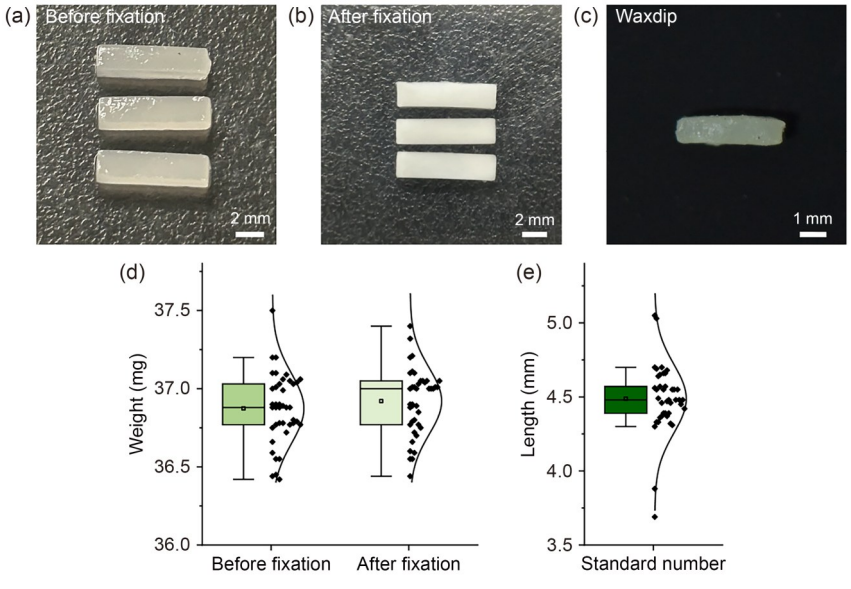

Fig. 3 Analysis of the appearance and quality of the organ model. The appearance of the model before (a) and after (b) fixation, and after deparaffinization (c). (d) Model weight comparison before and after fixation (n=41; p=0.33). (e) Length analysis of the model after dehydration and paraffin immersion (n=41)

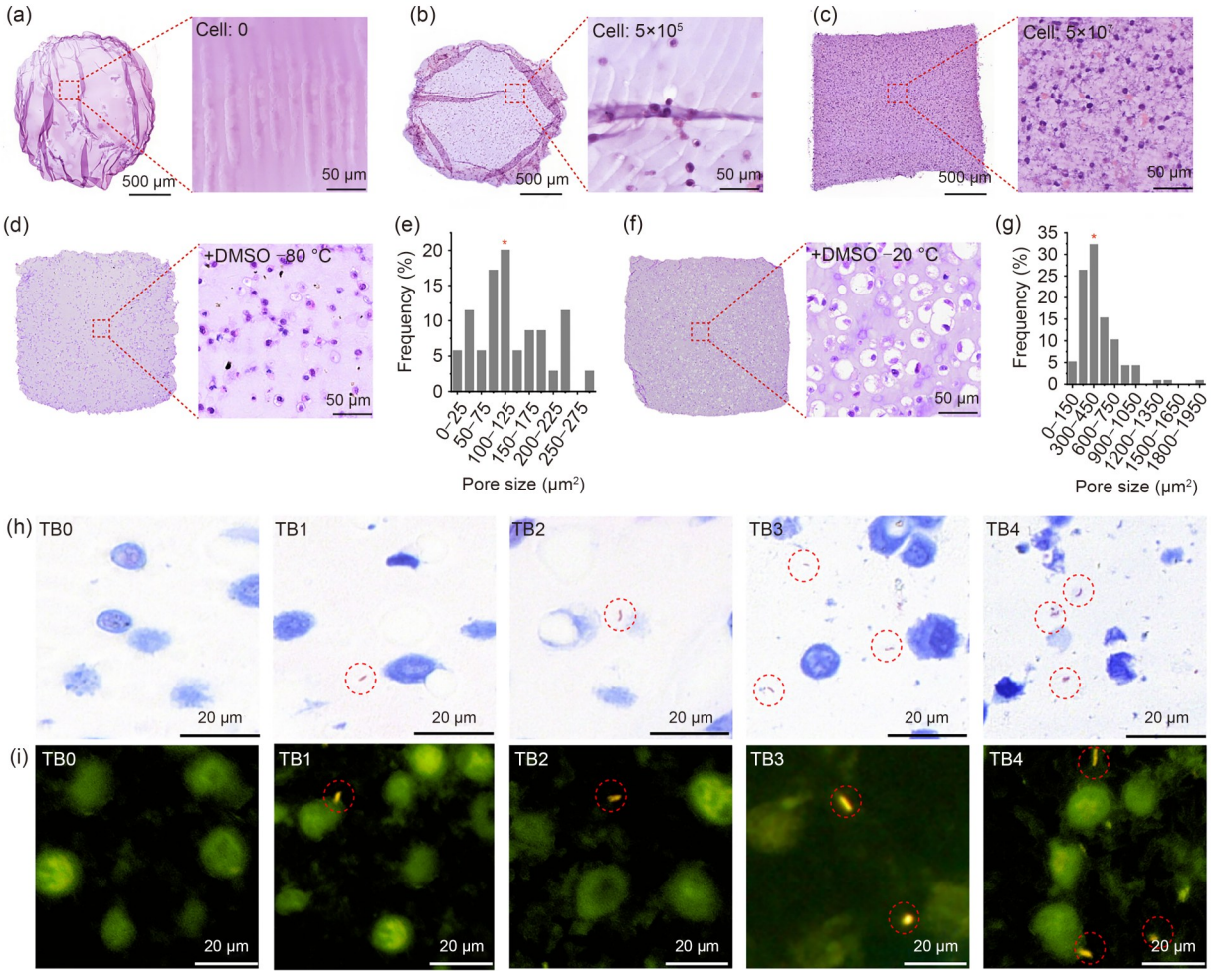

Fig. 4 Histological staining analysis and storage stability. H&E staining of samples without cells (a), with 5×10^5 cells/mL (b), and with 5×10^7 cells/mL (c) in the matrix. H&E staining (d, f) and cavity analysis (e, g) of samples stored at −80 and −20 °C for one month. AFB (h) and IF (i) staining of a negative control and four gradients of positive QC chips. * in (e, g) highlights the pore size with the highest frequency

observed with <300 μm^2 microcavities (Figs. 4d and 4e; Fig. S3d in the supplementary information). In the −20 °C group, cavities measuring 300–450 μm^2 were observed after one month, accounting for 32.5% of the observed area. These cavities were further enlarged after 12 months, resulting in significant structural damage (Figs. 4f and 4g; Fig. S3g in the supplementary information). The structural stability of the QC chips during the storage period is crucial for their subsequent applications. The structural fidelity of paraffin-embedded specimens and those stored at 80 °C can meet the requirements of subsequent application.

3.3.2 MTB quantification and stability assessment

To verify the homogeneity of MTB in the QC chips, we used a dual system consisting of AFB/IF staining. No MTB was detected in the TB0 group; the rest of the positive QC chips exhibited a uniform bacterial distribution under high magnification, without obvious aggregation, background staining, or bacterial fragments (Figs. 4h and 4i). Subsequently, the effects of long-term storage on morphology and counting were examined.

Morphology: After 12 months of QC microarray paraffin embedding and 12 months of freezing at −80 °C, the structure remained intact, AFB/IF positive localization was accurate, and cell structure was clear (Figs. S3b, S3c, S3e, and S3f in the supplementary information). After cryopreservation at −20 °C for 12 months, the tissues appeared significantly shrunken, with cavities and decreased structural integrity (Figs. S3h and S3i in the supplementary information).

Bacterial load: Compared with the control group, there was no statistically significant difference in MTB counts for the first four groups (paraffin/12 months, −80 °C/1 month, −80 °C/12 months, and −20 °C/1 month), but there was a significant difference for the −20 °C/12 months group (Fig. S4c in the supplementary information).

Linearity and batch-to-batch consistency: MTB density of TB1–TB4 chips was linearly correlated with initial bacterial concentration (Fig. S4d in the supplementary information).

Pairwise comparison of the four batches of TB3 chips showed no statistically significant difference in MTB count (p>0.05, Fig. S4e in the supplementary information), confirming accurate quantification and repeatability of the process.

3.4 Verification of the molecular performance of the QC chip

3.4.1 Intra-batch consistency

Intra-batch consistency was assessed by purifying nucleic acids and performing micro-UV detection. The OD_{260}/OD_{280} ratios for the five QC chips were as follows: TB0 (2.00±0.03), TB1 (1.95±0.01), TB2 (1.98±0.02), TB3 (1.93±0.01), and TB4 (1.93±0.02), with CV<5% (Fig. 5a). The nucleic acid concentrations in the QC chips were positively correlated with the HeLa cell concentrations (Fig. 5b). All five groups of the QC chips met the PCR acceptance criteria for FFPE tissues. The DNA concentrations of the five QC chips were as follows: TB0 ((26.98±0.33) ng/μL), TB1 ((27.80±0.33) ng/μL), TB2 ((26.37±0.51) ng/μL), TB3 ((27.83±0.41) ng/μL), and TB4 ((25.99±0.46) ng/μL), with CV<5% (Fig. 5c). The qPCR results showed that no S-shaped amplification occurred in either the negative control chip or the negative standard. The internal control curve as well as the positive standard sample results was normal (Fig. 5d). The amplification curves of the TB1–TB4 QC chips were normal, with CV values for C_t values all below 5%, as follows: TB1 (36.44±0.82, CV=2%); TB2 (33.42±0.57, CV=2%); TB3 (30.03±0.36, CV=1%); TB4 (26.27±0.36, CV=1%) (Figs. 5e–5h). The C_t values of TB0 to TB4 exhibited a good linear relationship. TB1–TB4 precisely matched the 10-fold dilution pattern (the difference in C_t values between adjacent gradients was approximately 3.14) (Fig. 5i). These results indicate that the constructed QC chip has good intra-assay consistency and a wide detection range, allowing the selection of an appropriate chip to validate the sensitivity and specificity of the experiment as needed.

3.4.2 Inter-batch consistency

To verify inter-batch consistency, we selected four independent batches of TB3, each with nine QC chips for molecular detection. The OD_{260}/OD_{280} ratios of the QC chips (36 cases) were all between 1.8 and 2.1 (Fig. 6a). The average DNA concentration was (27.24±1.15) ng/μL (CV=4.23%) (Fig. 6b).

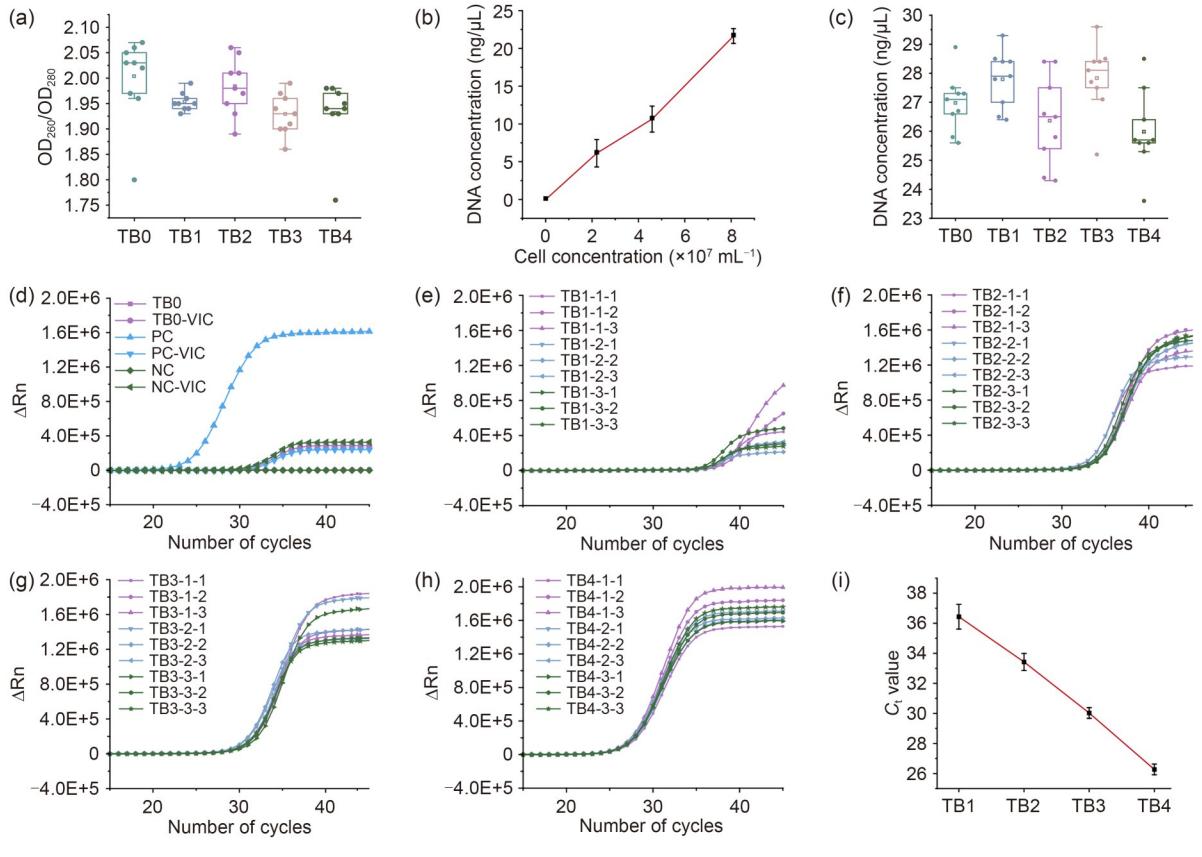

Fig. 5 Performance verification of the QC chip for each group. (a) OD_{260}/OD_{280} ratios. (b) Relationship between cell and DNA concentrations. (c) DNA concentrations of the TB0–TB4 QC chips. Amplification curves of (d) the positive and negative standards and negative QC chips, as well as (e–h) the TB1–TB4 QC chips. In qPCR, ΔRn refers to the magnitude of the normalized fluorescence signal generated by the reporter at each cycle during the PCR amplification process. (i) Comparison of C_t values across four gradient QC chips. Data in (b, i) are expressed as mean±standard deviation (n=9)

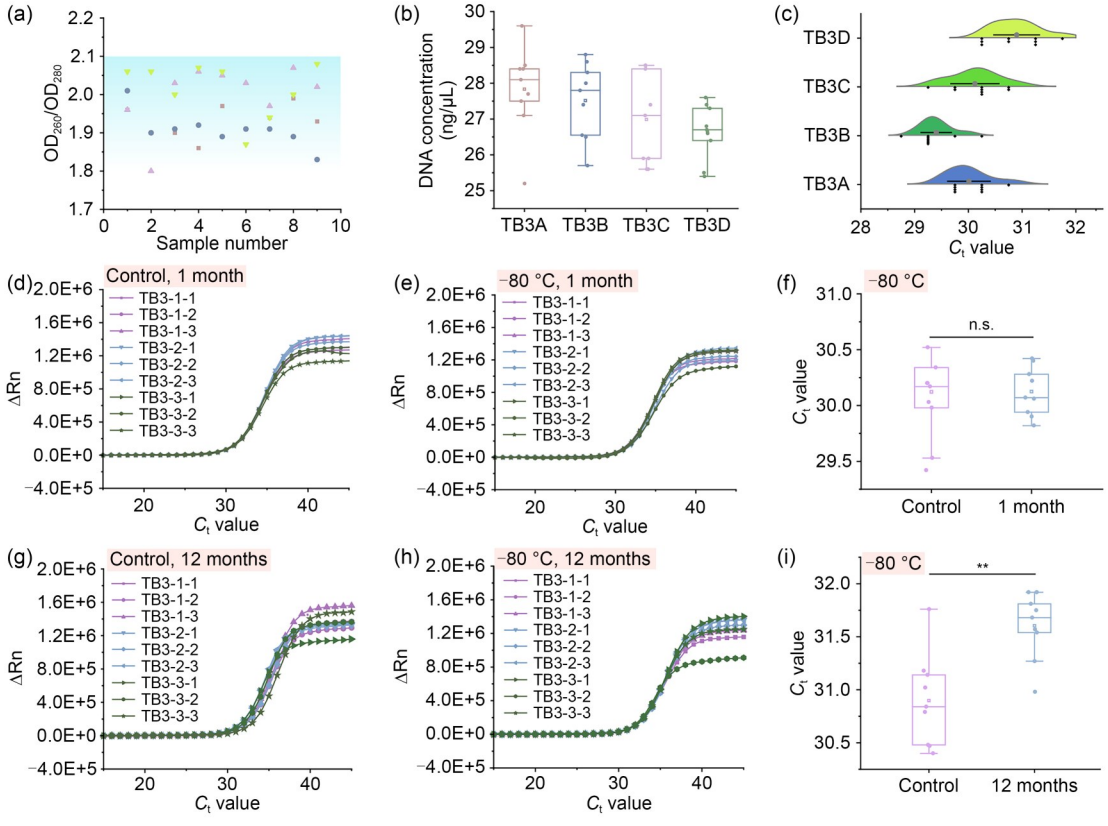

Fig. 6 Verification of inter-batch consistency and storage stability. (a) OD_{260}/OD_{280} values. (b) DNA concentrations (n=9). (c) C_t values of four batches of TB3 QC chips. Amplification curves of the control group (d) and QC chips stored at −80 °C for one month (e). In qPCR, ΔRn refers to the magnitude of the normalized fluorescence signal generated by the reporter at each cycle during the PCR amplification process. (f) Comparison of C_t values for QC chips stored at low temperature for 1 month, p=0.991 (n=9). Amplification curves of the control group (g) and QC chips stored at −80 °C for 12 months (h). (i) Comparison of C_t values for QC chips stored at −80 °C for 12 months, p=0.003 (n=9). $^{**}p<0.01$; n.s.: not significant

The average C_t values for the four batches of QC chips were 30.01±0.41, 29.40±0.29, 30.12±0.46, and 30.90±0.43, respectively (Fig. 6c). Statistical analysis revealed that only the difference between TB3A and TB3C was not statistically significant (p=0.59), while pairwise comparisons of all other batches showed statistical significance ($p<0.05$). However, the overall average C_t value for the 36 samples was 30.1±0.66 (CV=2.2%). Additionally, the maximum deviation in C_t values between batches was <1, indicating that observed differences may be attributed to random error and remain within an acceptable range. These findings demonstrate high consistency among different batches of QC chips, thereby enhancing data comparability and standardization of experimental methods.

3.4.3 DNA stability

To evaluate the stability of DNA storage, freshly demolded QC models were flash-frozen in liquid nitrogen for one minute and subsequently stored at −80 °C. Post-storage analysis revealed no significant degradation in DNA purity or concentration after 1 month and 12 months, with all samples remaining within acceptable detection limits (Fig. S5 in the supplementary information).

After one month of storage, the amplification curves and C_t values (30.12±0.15 for controls vs. 30.12±0.22 for −80 °C storage, p=0.99) showed no statistically significant differences between the control and −80 °C groups (Figs. 6d–6f). However, by 12 months, a slight but statistically significant divergence emerged (30.90±0.43 for controls vs. 31.60±0.31 for −80 °C storage, p=0.003), though the maximum C_t difference remained below 1 (Figs. 6g–6i). Upon assessing the stability of paraffin-embedded samples stored at room temperature for 6 and 12 months, no notable decline in DNA purity or concentration was observed, and C_t values remained comparable to baseline levels (Table S2 in the supplementary information).

3.5 Clinical applications

3.5.1 AFB staining

Using TB0 (negative) and TB4 (positive) QC chips as external QC references, the test tissues were pasted on the same glass slide for synchronous staining operations. QC of AFB staining was performed using 200 clinical FFPE tissue sections from Taizhou Hospital in Zhejiang Province. The TB0

chip remained negative in all cases, with 100% specificity, while the TB4 chip showed typical, red-stained bacilli in every case, with 100% sensitivity. The chip size is only 1 mm×1 mm, making it easy to distinguish from the tested tissue and eliminating ambiguity.

3.5.2 qPCR detection

In this study, the TB0 and TB2 QC chips and kit standards were used to evaluate the accuracy and reproducibility of qPCR detection using FFPE tissues. In the 12 test runs conducted, TB0 remained negative throughout, indicating no contamination, and the specificity reached 100%. However, the TB2 QC chip showed inconsistent results in the first six tests conducted by different operators: two negative, three positive, and one borderline result. The positive standard (plasmid DNA) yielded stable results (C_t=29.61±0.63, CV=2.16%). After optimizing the operational process (standardizing section thickness, improving dewaxing, implementing multi-step suction washing, and enhancing operator training), the subsequent six runs yielded 100% positive results for the TB2 chip, with C_t=36.67±0.93 (CV=2.55%). The respective reagent kit standard had a C_t value of 29.66±0.64 (CV=2.26%) (Fig. 7). To date, a comprehensive TB QC has been provided for 40 clinical samples, with a positive rate of 30% (12/40).

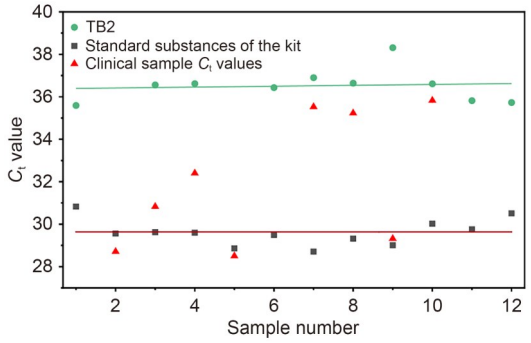

Fig. 7 C_t values of 12 clinical samples, TB2, and kit standards

4 Discussion

To our knowledge, this study is the first to report a quantitative, long-term storable QC chip for the entire process of MTB detection, which is suitable for histopathological staining and molecular detection. This system overcomes the shortcomings of reagent kit QC materials and facilitates the reproducibility of pathological detection methods for MTB.

It is imperative that the MTB (target) quantification of the QC chip is accurate and reproducible, and that the nucleic acid quality meets the entry criteria for PCR testing. The cells in the QC chip simulate actual tissues, ensuring that the processing time of the QC model is consistent with that of real tissue, as well as the accuracy of the nucleic acid extraction efficiency. Unlike existing organ/tissue chips that require recreating complex pathological environments, the QC chip does not need to reproduce the granulomatous microenvironment caused by MTB infection, and thus does not require specific cell types, such as lung epithelial cells. Therefore, the HeLa cells, which proliferate rapidly and have small batch-to-batch variability, were selected for this chip. An MTB QC strain with good stability and compliant with the ISO 17034 requirements was used as the target to improve sensitivity and enable specific assessments.

During the chip manufacturing process, low mechanical strength, susceptibility to cracking and deformation, and difficulty in dispersing MTB aggregates using traditional agar casting methods are some of the challenges. To overcome these, we systematically optimized the materials and methods. In the dispersion process, to avoid cell damage caused by ultrasonic mixing, we selected a 40-kHz ultrasonic water bath with gentle cavitation [13] and used 3 mm steel balls as resonance sources to amplify the ultrasonic effect within the container, thereby preventing conduction attenuation. The tank temperature was precisely controlled at (37±2) °C, resulting in a highly homogeneous matrix with excellent flowability. Furthermore, the QC model was cast with highly dispersed components.

The storage stability of the QC model directly determines its performance. If cryopreservation strategies used for biological samples are employed, the ice crystals formed during repeated freeze-thaw cycles may damage the structure of the QC models and the morphology of the cells/bacteria within them. The extent of this damage depends on the number of freeze-thaw cycles, the rate of temperature change, and the composition of the QC model [14]. Studies have shown that the use of DMSO for vitrification and rapid cryopreservation of biological materials at ultra-low temperatures can help inhibit ice crystal formation [15]. Therefore, we adopted a triple strategy of "10% (volume fraction) DMSO + liquid nitrogen rapid freezing + −80 °C low-temperature storage": DMSO stabilizes cell membranes, vitrification prevents ice crystal formation, and rapid freezing and deep low temperatures further mitigate damage. The QC chips stored under these conditions showed no significant changes in staining performance or DNA quality after over 12 months. Another common storage method is paraffin embedding. The physical barrier effect of wax effectively prevents water migration and oxidation, thereby maintaining the integrity of the pore structure and the stability of antigens/nucleic acids [16]. Once the QC model is cast into a wax block, it can be stored at room temperature for an extended period (over 12 months) without requiring low-temperature facilities. A single-pour QC model can be stored for long-term use, enabling different laboratories to utilize QC products of consistent quality over an extended

period, thereby facilitating cross-laboratory data comparison and result sharing.

In clinical practice, AFB is the primary screening method for TB due to its low cost and rapid results. However, its low detection rate (sensitivity of only 12.0%–30.8%) often necessitates the use of secondary staining methods [17]. External controls are often required to ensure the reliability of staining. The novel QC chip provides accurate quantitative results and can be used for simultaneous staining and diagnosis with the tested tissue. It overcomes the drawbacks of traditional positive archival wax blocks, which have uneven bacterial loads, poor reproducibility, and ethical concerns. Herein, we conducted a full-process QC on 200 special staining cases, and the results showed that the staining was accurate and reliable, requiring no further verification.

In laboratories that have passed clinical PCR certification, qPCR is considered the best method for detecting MTB in FFPE tissues [18], with a sensitivity of approximately 50%−84%, which is several times higher than that of AFB staining. However, its operational steps are cumbersome and subject to numerous influencing factors. The Clinical and Laboratory Standards Institute recommends using QC materials with matrix components identical to the test samples to implement comprehensive QC for nucleic acid testing, thereby minimizing the risk of false positives or negatives.

Furthermore, we used flow cytometry to accurately quantify the MTB content in four positive gradient QC chips, resulting in reliable calibration curves that meet daily QC needs and can also serve as a unified interlaboratory quality assessment standard for the National Pathology Quality Control Center, with broad application prospects. Due to recent advancements in biological 3D printing, the manufacturing of QC can be further automated and standardized if precise light field control, precise ink response, and mechanical balance maintenance can be achieved [19–21].

5 Conclusions

The QC-chip system developed herein covered the entire process of MTB testing. This QC chip exhibited excellent consistency and stability, achieving a uniform gradient distribution of MTB and providing a reliable reference for the MTB detection workflow. This solid-state QC model was highly compatible with the processing program for detecting bacterial infections within tissues, overcoming the technical bottlenecks related to liquid standard materials in various detection kits, such as nucleic acid crosslinking, which can result in tissue disruption and degradation. A naturally occurring whole-genome MTB strain was adopted as the QC material, achieving compatibility with mainstream special staining techniques and nucleic acid amplification detection kits. Furthermore, the sensitivity and stability of this method were comprehensively assessed to ensure that it serves as a valuable tool for comparing results among laboratories. Furthermore, due to the uniform and controllable distribution of MTB, the QC chip offers a wide detection range, overcoming the limitations of existing detection methods. Overall, in addition to optimizing the entire MTB detection process, the proposed QC chip significantly improved the accuracy of sample detection, enabling timely and accurate clinical diagnosis. Furthermore, it can serve as a practical tool for training relevant technical personnel.

In summary, a novel QC chip was developed to enhance the reliability of the clinical pathological test workflow. This research incorporated clinically isolated strains to standardize MTB detection across different bacterial communities and various culture batches, as well as drug-resistant MTB strains, to further improve the QC system.

Supplementary Information The online version contains supplementary material available at https://doi.org/10.1631/bdm.2500274.

Acknowledgements This work was supported by the National Natural Science Foundation of China (Nos. 52325504 and 52235007), the Basic Public Welfare Research Project of Zhejiang Province (No. LGY23H160089), and the Science and Technology Plan Project of Taizhou City (No. 24ywa08).

Author contributions Conceptualization: YH, JX, and MFG. Investigation: ERY, JH, LNZ, and JX. Resources: CFH, JX, QJZ, and LNZ. Writing—original draft: ERY, JH, and JX. Writing—review & editing: YH, JX, MFG, and CFH. Visualization: ERY, JX, JH, and CFH. Funding acquisition: YH, JX, and ERY. Supervision: YH.

Declarations

Conflict of interest YH is an associate editor for *Bio-Design and Manufacturing* and was not involved in the editorial review or the decision to publish this article. The authors declare that they have no conflict of interest.

Ethical approval This study utilized human clinical samples, and all experiments were conducted in accordance with the Declaration of Helsinki, International Conference on Harmonization Good Clinical Practice (ICH-GCP) guidelines. The experimental protocol was approved by the Medical Ethics Committee of Taizhou Hospital of Zhejiang Province (Approval No. K20250330). Written informed consent (both for participation and publication) was obtained from each patient or the patient's legal guardian.

Data availability All data supporting the findings of this study are available within the article and its supplementary files. Any additional requests for information can be directed to the corresponding authors, who will fulfill them.

References

1. Bagcchi S (2023) WHO's global tuberculosis report 2022. Lancet Microbe 4(1):e20. https://doi.org/10.1016/S2666-5247(22)00359-7
2. He G, Chen CY, Zhang X et al (2022) Clinical performance of quantitative PCR for the molecular identification of skeletal tuberculosis from formalin-fixed paraffin-embedded tissues. BMC Infect Dis 22(1):651. https://doi.org/10.1186/s12879-022-07641-7
3. Meireles SI, Cruz MV, Irffi GP et al (2024) Incidence of mycobacteria in pulmonary granulomatous lesions. Clinics 80:100564. https://doi.org/10.1016/j.clinsp.2024.100564
4. Hou XF, Guo QL, Lin Q et al (2022) Determination of the predictive factors for diagnostic positivity of nucleic acid amplification tests for diagnosing pulmonary tuberculosis. Infect Med 1(1): 17–22. https://doi.org/10.1016/j.imj.2022.02.003
5. Eddabra R, Ait Benhassou H (2018) Rapid molecular assays for detection of tuberculosis. Pneumonia 10:4. https://doi.org/10.1186/s41479-018-0049-2
6. Steiert TA, Parra G, Gut M et al (2023) A critical spotlight on the paradigms of FFPE-DNA sequencing. Nucleic Acids Res 51(14):7143–7162. https://doi.org/10.1093/nar/gkad519
7. Okubo Y, Toyama N, Kasajima R et al (2024) Effective preparation of FFPE tissue samples for preserving appropriate nucleic acid quality for genomic analysis in thyroid carcinoma. Endocr Pathol 35(4):372–384. https://doi.org/10.1007/s12022-024-09838-9
8. Flores Bueso Y, Walker SP, Hogan G et al (2020) Protoblock - a biological standard for formalin fixed samples. Microbiome 8(1): 122. https://doi.org/10.1186/s40168-020-00901-1
9. Ingber DE (2022) Human organs-on-chips for disease modelling, drug development and personalized medicine. Nat Rev Genet 23(8): 467–491. https://doi.org/10.1038/s41576-022-00466-9
10. Alonso-Roman R, Mosig AS, Figge MT et al (2024) Organ-on-chip models for infectious disease research. Nat Microbiol 9(4): 891–904. https://doi.org/10.1038/s41564-024-01645-6
11. He J, Sun Y, Gao Q et al (2023) Gelatin methacryloyl hydrogel, from standardization, performance, to biomedical application. Adv Healthc Mater 12(23):2300395. https://doi.org/10.1002/adhm.202300395
12. Lin M, Cao HS, Li JM (2023) Control strategies of ice nucleation, growth, and recrystallization for cryopreservation. Acta Biomater 155:35–56. https://doi.org/10.1016/j.actbio.2022.10.056
13. Gehrke P, Smeets R, Gosau M et al (2019) The influence of an ultrasonic cleaning protocol for CAD/CAM abutment surfaces on cell viability and inflammatory response in vitro. In Vivo 33(3): 689–698. https://doi.org/10.21873/invivo.11527
14. Lee E, Baiz CR (2022) How cryoprotectants work: hydrogen-bonding in low-temperature vitrified solutions. Chem Sci 13(34): 9980–9984. https://doi.org/10.1039/D2SC03188D
15. Mashouf P, Tabibzadeh N, Kuraoka S et al (2024) Cryopreservation of human kidney organoids. Cell Mol Life Sci 81(1):306. https://doi.org/10.1007/s00018-024-05352-7
16. Groelz D, Viertler C, Pabst D et al (2018) Impact of storage conditions on the quality of nucleic acids in paraffin embedded tissues. PLoS ONE 13(9):e0203608. https://doi.org/10.1371/journal.pone.0203608
17. Acharya B, Acharya A, Gautam S et al (2020) Advances in diagnosis of tuberculosis: an update into molecular diagnosis of *Mycobacterium* tuberculosis. Mol Biol Rep 47(5):4065–4075. https://doi.org/10.1007/s11033-020-05413-7
18. Burkardt HJ (2000) Standardization and quality control of PCR analyses. Clin Chem Lab Med 38(2):87–91. https://doi.org/10.1515/CCLM.2000.014
19. He CF, Qiao TH, Ren XC et al (2025) Printability in multi-material projection-based 3-dimensional bioprinting. Research 8:0613. https://doi.org/10.34133/research.0613
20. Cao Q, Zhang Y, Deng R et al (2023) Biomanufacturing in Japan: frontier research from 2018 to 2023. Bio-Des Manuf 6(6):617–645. https://doi.org/10.1007/s42242-023-00261-3
21. He CF, He JK, Wu CT et al (2025) 3D printing for tissue/organ regeneration in China. Bio-Des Manuf 8(2):169–242. https://doi.org/10.1631/bdm.2400309